
SOLVING LARGE FLEXIBLE JOB SHOP SCHEDULING INSTANCES BY GENERATING A DIVERSE SET OF SCHEDULING POLICIES WITH DEEP REINFORCEMENT LEARNING

Imanol Echeverria*

TECNALIA, Basque Research and Technology Alliance (BRTA)
Mikeletegi Pasealeakua 7, 20009 Donostia-San Sebastián (Spain)
imanol.echeverria@tecnalia.com

Maialen Murua

TECNALIA, Basque Research and Technology Alliance (BRTA)
Mikeletegi Pasealeakua 7, 20009 Donostia-San Sebastián (Spain)
maialen.murua@tecnalia.com

Roberto Santana

Computer Science and Artificial Intelligence Department
University of the Basque Country
Lardizabal Pasealeakua 1, 20018 Donostia-San Sebastián (Spain).
roberto.santana@ehu.eus

ABSTRACT

The Flexible Job Shop Scheduling Problem (FJSSP) has been extensively studied in the literature, and multiple approaches have been proposed within the heuristic, exact, and metaheuristic methods. However, the industry's demand to be able to respond in real-time to disruptive events has generated the necessity to be able to generate new schedules within a few seconds. Among these methods, under this constraint, only dispatching rules (DRs) are capable of generating schedules, even though their quality can be improved. To improve the results, recent methods have been proposed for modeling the FJSSP as a Markov Decision Process (MDP) and employing reinforcement learning to create a policy that generates an optimal solution assigning operations to machines. Nonetheless, there is still room for improvement, particularly in the larger FJSSP instances which are common in real-world scenarios. Therefore, the objective of this paper is to propose a method capable of robustly solving large instances of the FJSSP. To achieve this, we propose a novel way of modeling the FJSSP as an MDP using graph neural networks. We also present two methods to make inference more robust: generating a diverse set of scheduling policies that can be parallelized and limiting them using DRs. We have tested our approach on synthetically generated instances and various public benchmarks and found that our approach outperforms dispatching rules and achieves better results than three other recent deep reinforcement learning methods on larger FJSSP instances.

Keywords Flexible job shop scheduling · Deep reinforcement learning · Heterogeneous graph neural networks · Markov decision process

1 Introduction

Planning consists of assigning a series of operations to a set of resources within a specified time period to optimize one or multiple objectives. It is a widely studied problem in the literature due to its impact on the manufacturing industry (Gupta and Sivakumar, 2006) and various other real-world scenarios (Çaliş and Bulkan, 2015). One of the

*Corresponding author.

most well-known variants is the job shop scheduling problem (JSSP) (Manne, 1960), in which a set of jobs, composed of operations, must be assigned to a set of machines. Each one of these operations can only be performed on a single given machine, and the order of the operations within a job must be respected. The objective of the problem is to create a resource allocation that optimizes one or multiple key performance indicators, with makespan being the most commonly used in the literature, defined as the time to complete all operations, as well as other metrics related to job tardiness or production costs such as energy consumption (Xiong et al., 2022). Due to its complexity, this problem is known to be NP-Hard (Garey et al., 1976). A well-studied extension of the JSSP is the Flexible Job Shop Scheduling Problem (FJSSP), where the difference lies in the fact that each one of the operations can be processed on a set of machines instead of a single one. This problem is also NP-Hard as it adds the complexity of determining the optimal route for operations, resulting in a significantly larger search space of possible solutions.

Multiple approaches have been proposed in the literature to find optimal solutions for the FJSSP. Within the family of exact optimization methods, dynamic programming-based methods have been proposed (Kim et al., 2022), although the most common ones are based on linear programming or mixed linear programming (Meng et al., 2020; Tutumlu and Saraç, 2023). However, due to the NP-hardness of the FJSSP, these methods cannot handle medium-large instances of the problem in a dynamic manner, that is, cannot generate optimal or pseudo-optimal solutions in real-time, and the sizes of the instances typically used for benchmarking are much smaller than those encountered in real-world scenarios. For example, in Meng et al. (2020), the authors use the first ten instances from the well-known Brandimarte benchmark (Brandimarte, 1993), with the largest instance consisting of only twenty jobs and fifteen machines. This size is much smaller compared to real-world scenarios found in the industry, which can involve hundreds or thousands of jobs and dozens of machines.

On the other hand, metaheuristic algorithms, particularly genetic algorithms (Zhang et al., 2020b; Chen et al., 2020), as well as approaches based on tabu search (Hajibabaei and Behnamian, 2021) or simulated annealing (Defersha et al., 2022), have been widely employed. Although metaheuristic methods are more efficient than exact methods, both require a considerable amount of time to obtain satisfactory solutions as the algorithms need to iterate to find these solutions. Therefore, neither of these two approaches is suitable for environments with disruptive events, such as machine breakdowns or new jobs that need to be accommodated in real-time. Dispatching rules (DRs) (Calleja and Pastor, 2014; Chen and Matis, 2013), methods framed within the family of heuristics, are the most commonly used options in such situations. These rules consist of two criteria: the sequencing order of operations and the assignment of each operation to a machine. They also have the advantage of being capable of generating solutions quickly for large instances of the FJSSP. However, they present some disadvantages. Both criteria need to be manually designed by an expert, which requires time and effort, and they are also static, making them strategies that cannot adapt to diverse problem instances and cannot find global optimal solutions (Luo et al., 2021).

Reinforcement learning (RL) and deep reinforcement learning (DRL) have emerged as promising alternatives to tackle problems that can be modeled as a Markov Decision Process (MDP), including other NP-Hard problems such as the Traveling Salesman Problem (Cappart et al., 2021; Mazyavkina et al., 2021) or the Vehicle Routing Problem (Joe and Lau, 2020). Scheduling problems such as the FJSSP have received less attention in the literature but, in recent years, various DRL approaches have been proposed to tackle the JSSP and the FJSSP, with the former being more common due to be easier to model. To apply RL to scheduling problems, the problem is first modeled as an MDP, and RL algorithms are used to learn a policy that sequentially assigns operations to machines while attempting to maximize the accumulated reward, which is usually designed to minimize the makespan.

In general, the proposed DRL approaches outperform DRs, but there are still limitations that need to be addressed to apply these methods in real-world scenarios. One significant difference between current approaches and real-world scenarios is the size of the benchmarks. For instance, in Song et al. (2022) and Wang et al. (2023), two benchmark sets were used: the first ten instances from Brandimarte (Brandimarte, 1993) and the sets of instances proposed by Hurink (the rdata, vdata, and edata sets) (Hurink et al., 1994), with a maximum of twenty machines and thirty jobs. These instance sets have a limited number of elements compared to real-world scenarios, where there can be thousands of jobs and dozens of machines. In this regard, Behnke and Geiger (2012) proposed a benchmark of more realistic instances of larger sizes, with up to one hundred jobs and sixty machines, which is utilized by Lei et al. (2022) in their approach, in addition to the vdata set to evaluate the performance on smaller instances. Although near-optimal results can be obtained on small instances, there is more room for improvement on large instances. Therefore, the objective of this paper is to propose a novel end-to-end DRL framework that robustly solves FJSSP instances, outperforming DRs and recent DRL-based methods. The aim is to narrow the gap between instances typically used in the literature and problems that resemble real-world scenarios. The contributions of this paper can be summarized as follows:

- A novel representation of the state space is achieved by minimizing the required information and appropriately distributing it among three types of nodes (jobs, operations, and machines), along with a set of edges that facilitate the transmission of information between nodes. As the instance progresses, unnecessary edges and nodes are eliminated to enhance the efficiency of the training and inference phases.
- Limiting the action space using masks and employing DRs to achieve faster model training and more robust inference behavior.
- A method for generating a diverse set of scheduling policies through Bayesian optimization and a method for selecting the best policies using K -Nearest Neighbors, efficiently parallelizing models during inference to improve performance.

2 Preliminaries

In this section, we will briefly describe how the FJSSP is formulated, as well as introducing key concepts of RL and Graph Neural Networks (GNNs) that will be used in our proposed method.

2.1 Problem formulation

An instance of the FJSSP problem is defined by a set of jobs $\mathcal{J} = \{j_1, j_2, \dots, j_n\}$, where each $j_i \in \mathcal{J}$ is composed of a set of operations $\mathcal{O}_{j_i} = \{o_{i1}, o_{i2}, \dots, o_{im}\}$, and each operation can be performed on one or more machines from the set $\mathcal{M} = \{m_1, m_2, \dots, m_p\}$. The processing time of operation o_{ij} on machine m_k is defined as $p_{ijk} \in \mathbb{R}^+$. We define $\mathcal{M}_{o_{ij}} \subseteq \mathcal{M}$ as the subset of machines on which that operation o_{ij} can be processed, $\mathcal{O}_{j_i} \subseteq \mathcal{O}$ as the set of operations that belong to the job j_i where $\bigcup_{i=1}^n \mathcal{O}_{j_i} = \mathcal{O}$, and $\mathcal{O}_{m_k} \subseteq \mathcal{O}$ as the set of operations that can be performed on machine m_k . The execution of operations on machines must satisfy a series of constraints:

- All machines and jobs are available at time zero.
- A machine can only execute one operation at a time, and the execution cannot be interrupted.
- An operation can only be performed on one machine at a time.
- The execution order of the set of operations \mathcal{O}_{j_i} for every $j_i \in \mathcal{J}$ must be respected.
- Job executions are independent of each other, meaning no operation from any job precedes or has priority over the operation of another job.

In essence, the FJSSP combines two problems: a machine selection problem, where the most suitable machine is chosen for each operation, a routing problem, and a sequencing or scheduling problem, where the sequence of operations on a machine needs to be determined. Given an assignment of operations to machines, the completion time of a job, j_i , is defined as C_{j_i} , and the makespan of a schedule is defined as $C_{max} = \max_{j_i \in \mathcal{J}} C_{j_i}$, which is the most common objective to minimize.

2.2 Reinforcement Learning and Proximal Policy Optimization

MDPs provide a mathematical framework for modeling decision-making processes. Formally, a MDP is defined as a tuple $(\mathcal{S}, \mathcal{A}, R, P)$, where \mathcal{S} is a finite set of elements called states, \mathcal{A} is a finite set of elements called actions, $R : \mathcal{S} \times \mathcal{A} \rightarrow \mathbb{R}$ represents the reward the agent receives when taking action a in state s , and P is a function $P : \mathcal{S} \times \mathcal{A} \times \mathcal{S} \rightarrow [0, 1]$ that represents the probability of transitioning from state s to s' when taking action a . The goal of RL is to learn a policy $\pi_\theta : \mathcal{S} \times \mathcal{A} \rightarrow [0, 1]$, which is parameterized by θ , in order to maximize the expected cumulative reward by mapping states to actions (Sutton and Barto, 2018). The future rewards that the agent receives are usually multiplied by a discount factor $\gamma \in [0, 1]$.

There are multiple algorithms to find the parameters θ that generate an optimal policy, and one of the most widely used is Proximal Policy Optimization (PPO) (Schulman et al., 2017). PPO iteratively updates the policy using a surrogate objective function based on the advantage function. The advantage function, denoted by $A : \mathcal{S} \times \mathcal{A} \rightarrow \mathbb{R}$, measures how good an action is compared to the average of all possible actions in a particular state. The surrogate objective function encourages policy updates that increase the probability of actions that maximize the expected cumulative reward. At time step t , the policy will be updated to minimize the defined loss function:

$$L^{CLIP}(\theta) = \hat{E}_t \left[\min \left(r_t(\theta) \hat{A}_t, \text{clip} \left(r_t(\theta), 1 - \varepsilon, 1 + \varepsilon \right) \hat{A}_t \right) \right] \quad (1)$$

where \hat{E}_t denotes the empirical expectation over future time steps, \hat{A}_t represents the empirical advantage, r_t is the ratio of change between the current policy and the previous policy, the function clip restricts the value of the first parameter within the range defined by the second and third parameters it receives, and ε is a hyperparameter (usually 0.1 or 0.2) that is used in the clip function and determines the extent to which the policy is allowed to be updated.

2.3 Graph Neural Networks

GNNs (Scarselli et al., 2008) have received significant attention in recent years (Zhang et al., 2021; Zhou et al., 2020) due to their ability to efficiently extract information from structured data in the form of graphs, where predictions are made based on the edges connecting the nodes. A directed graph \mathcal{G} is defined as a tuple of two sets $(\mathcal{V}, \mathcal{E})$ where \mathcal{V} contains nodes, $\mathcal{V} = \{1, \dots, n\}$, and \mathcal{E} edges, $\mathcal{E} \subseteq \mathcal{V} \times \mathcal{V}$, where $(i, j) \in \mathcal{E}$ represents an edge from a node i to a node j . It is assumed that every node has an initial representation $\mathbf{h}_i^{(0)} \in \mathbb{R}^{d_0}$, where d_0 is the number of the initial features of the node, and that all edges are directed, so an undirected graph can be represented with bidirectional edges. Multiple GNN architectures have been proposed (Wu et al., 2020), but one of the most commonly used ones is the Graph Attention Network (GAT) (Veličković et al., 2017), where each node updates its representation by aggregating the representations of its neighbors. Specifically, given a set of node representations $\mathcal{H} = \{\mathbf{h}_1, \mathbf{h}_2 \dots \mathbf{h}_n\}$, the update of the representation of a node \mathbf{h}_i is performed as follows:

$$\mathbf{h}_i' = f_\theta(\mathbf{h}_i, \text{AGGREGATE}(\{\mathbf{h}_j \mid j \in \mathcal{N}_i\})) \quad (2)$$

where \mathcal{N}_i represents the set of nodes connected to node i , while f and AGGREGATE are functions that define the GNN architecture. Many GNNs assign equal importance to all neighboring nodes, but in Veličković et al. (2017), the authors proposed a weighted average of the representations of \mathcal{N}_i through a scoring function that learns the importance of node j 's features to node i . The scoring function is defined as:

$$e(\mathbf{h}_i, \mathbf{h}_j) = \text{LeakyReLU}(\mathbf{a}^\top \cdot [\mathbf{W}\mathbf{h}_i \parallel \mathbf{W}\mathbf{h}_j]) \quad (3)$$

where $\mathbf{a} \in \mathbb{R}^{2d'}$ and $\mathbf{W} \in \mathbb{R}^{d' \times d_0}$ are learned vectors, d' is the length of the vector \mathbf{h}_i' and \parallel denotes vector concatenation. These scores are then normalized using the softmax function across all neighbors of the node, resulting in:

$$\alpha_{ij} = \text{softmax}_j(e(\mathbf{h}_i, \mathbf{h}_j)) = \frac{\exp(e(\mathbf{h}_i, \mathbf{h}_j))}{\sum_{j' \in \mathcal{N}_i} \exp(e(\mathbf{h}_i, \mathbf{h}_{j'}))} \quad (4)$$

Finally, to obtain \mathbf{h}_i' , a weighted sum of the representation of neighboring nodes is computed using the attention coefficients, followed by a non-linear activation function σ :

$$\mathbf{h}_i' = \sigma\left(\sum_{j \in \mathcal{N}_i} \alpha_{ij} \cdot \mathbf{W}\mathbf{h}_j\right) \quad (5)$$

Brody et al. (2021) proposed GATv2, which introduces a change in the internal order of these operations to achieve a more expressive attention mechanism. The problem with the original order is that the vectors \mathbf{W} and \mathbf{a} are applied consecutively, leading to them being collapsed into a single linear layer. The proposed solution is to apply \mathbf{a} after the non-linear function and \mathbf{W} after the concatenation, resulting in a more expressive score for each node-key pair. The updated formula becomes:

$$e(\mathbf{h}_i, \mathbf{h}_j) = \mathbf{a}^\top \text{LeakyReLU}(\mathbf{W} \cdot [\mathbf{h}_i \parallel \mathbf{h}_j]) \quad (6)$$

and \mathbf{W} can be divided into $[\mathbf{W}_1 \parallel \mathbf{W}_2] \mathbf{W}_1, \mathbf{W}_2 \in \mathbb{R}^{d' \times d}$ where each matrix represents the left half and right half of the columns of \mathbf{W} .

3 Related work

In this section, we will provide a brief analysis of the proposed methods for addressing the JSSP and the FJSSP, focusing on how they represent states and the algorithms they use to learn the scheduling policy.

Among the works addressing the JSSP, in Lin et al. (2019) a framework was proposed for smart manufacturing based on an off-policy RL method, deep Q-network (DQN), and edge computing is proposed to address the decisions of multiple edge devices. They encapsulate the state information into a feature vector that captures the relevant production state information and they employ a multilayer perceptron (MLP) to determine the value of a state. Similarly, in Luo (2020), a deep Q-network is employed to extract information from the production status using seven features that are used to select from six composite DRs. Instead of using vectors and off-policy methods, Liu et al. (2020) used

convolutional neural networks (CNNs) and the deep deterministic policy gradient (DDPG) algorithm, which belongs to the actor-critic family, was employed to tackle the problem. In this case, the input values are not a vector but a matrix with three channels: the first channel contains the process times of the operations, the second channel contains information about whether a job has been assigned to a machine, and the third channel indicates whether a job has been completed. This approach has the advantage of not having to design complicated features that reflect the production state, which can be time-consuming. One of the major drawbacks of these approaches is that they are not size-agnostic, meaning that the number of jobs or machines must be fixed since the inputs and outputs of an MLP cannot be variable. Additionally, much of the information in the JSSP, especially in the FJSSP, lies in its structure and the relationship between operations and machines, which is not directly encapsulated in these state representations.

Building upon the work done in other domains such as vehicle routing (Tolstaya et al., 2021), the information of a state can be represented using a graph, where nodes possess features that reflect their state and share information with connected nodes through edges. The state information can be extracted using GNNs and attention mechanisms (Vaswani et al., 2017; Veličković et al., 2017), which, unlike MLPs and CNNs, allow for capturing the structure of the state and its relationships. Moreover, they are size-agnostic, meaning the number of nodes in the problem is irrelevant. One way to represent JSSP and FJSSP is through a disjunctive graph (Balas, 1969), where nodes represent operations and two types of edges are employed. Directed edges indicate precedence among operations belonging to the same job, while undirected edges connect pairs of operations that can be performed on the same machine. With this representation, a solution is defined as an acyclic orientation of the undirected edges.

Using this representation, Zhang et al. (2020a) proposed a method to learn DRs using an end-to-end DRL agent for the JSSP using the PPO algorithm to train the policy. Song et al. (2022) extended this work to the FJSSP using a Heterogeneous GNN to capture state information and the relationships between operation and machine nodes. The authors in Lei et al. (2022) proposed to model the FJSSP as a multiple MDP, and multi-pointer graph networks which is a GNN that is employed to learn two sub-policies: one for operation selection and another for machine assignment. Wang et al. (2023) used attention models for deep feature extraction using a dual-attention network with operation message attention blocks and machine message attention blocks. Lastly, Du et al. (2022) modeled the multi-objective FJSSP with crane transportation and setup times, and total processing time and total energy consumption are optimized using a DQN model.

4 Proposed method

In this section, we will describe the proposed method to dynamically solve the FJSSP. First, we will explain how we have formulated the problem as an MDP, defining the state space, the action space, the reward function and state transitions. Secondly, we will present how we have modeled the policy using a GNN based on attention mechanisms and message passing between different nodes. Thirdly, we will describe two methods to make these approaches more robust, particularly in large instances, by applying masks based on DRs and using a novel method for generating a diverse set of scheduling policies.

4.1 The FJSSP as a Markov Decision Process.

To define an MDP, we need to specify the space of states, the action space, the reward and the state transitions. In broad terms, at each step, when an operation is completed, the agent must decide which operation to perform next and in which machine.

State space. Each state, which at step t is denoted as s_t , is a heterogeneous graph $\mathcal{G}_t = (\mathcal{V}_t, \mathcal{E}_t)$, where the set \mathcal{V}_t consists of three types of nodes: the set of operations \mathcal{O}_t , the set of machines \mathcal{M}_t , and the set of jobs \mathcal{J}_t . Each of these types of nodes has the following features:

- The operation nodes have a boolean feature indicating whether the operation can be performed or not and the pending processing time. For an operation, it is calculated as the sum of the average processing times of the remaining operations.
- The machine nodes have two features: the time at which the last assigned operation on the machine is completed and the utilization percentage of that machine.
- The features of job nodes contain most of the information. Their features include whether the job has been completed, the time at which its last assigned operation is finished, the number of operations remaining for that job and the pending processing time.

The set of edges \mathcal{E}_t consists of the following types of edges:

- Undirected edges between machines and operations, connecting operations that can be executed in machines and indicating their processing time. An undirected edge can be represented with two sets of directed edges, one between the operations and the machines, $\mathcal{OM}_t \subseteq \mathcal{O}_t \times \mathcal{M}_t$, and another between the machines and the operations, $\mathcal{MO}_t \subseteq \mathcal{M}_t \times \mathcal{O}_t$. Both have features which are the processing time, the ratio of the processing time to the maximum processing time of the operation and the ratio to the maximum of all the options that the machine can process.
- Directed edges between operations and jobs, indicating that an operation belongs to a job, $\mathcal{OJ}_t \subseteq \mathcal{O}_t \times \mathcal{J}_t$.
- Directed edges between operations, indicating that an operation immediately precedes the other, $\mathcal{OO}_t \subseteq \mathcal{O}_t \times \mathcal{O}_t$.
- Directed edges between machines and jobs, adding the processing time and the gap that would be generated by executing that job (i.e., the first operation that can be performed for that job) on that machine. It also has as features the same ratios as the edges between the operations and machines. The set of edges is defined as $\mathcal{MJ}_t \subseteq \mathcal{M}_t \times \mathcal{J}_t$ and each edge $(m_k, j_i) \in \mathcal{MJ}_t$ have features defined as pg_{ki} .
- Jobs are connected to each other to enable information communication among their states, $\mathcal{JJ}_t \subseteq \mathcal{J}_t \times \mathcal{J}_t$.
- Machines are connected to each other to enable information communication among their states, $\mathcal{MM}_t \subseteq \mathcal{M}_t \times \mathcal{M}_t$.

It should be noted that in our case, the number of features associated with nodes is reduced, resulting in a lower computational cost as less information needs to be calculated at each state. In comparison, in Song et al. (2022), operations have six features and machines have three features and in Wang et al. (2023) operations have ten features, machines eight and compatible operation-machine pairs also eight features.

Furthermore, the inclusion of a job node offers two main advantages. Firstly, it significantly reduces the action space, as the number of jobs is usually much smaller than the number of operations. Secondly, it concentrates the relevant information of the problem into a single type of node, making the learning process more efficient and the inference faster.

Action space. At each step t , the set of actions \mathcal{A}_t is composed of all pairs of compatible jobs and machines. When choosing a job, the first operation of the job that has not yet been scheduled is selected. This set corresponds to the set of edges that connect jobs and machines, \mathcal{MJ}_t . As explained in the next section, to improve learning efficiency and stabilize inference, based on a DR, some of these actions will be excluded from being eligible by the policy.

State Transitions. Since the MDP formulation of the FJSSP is deterministic, performing an action a_t in state s_t transitions to a new state s_{t+1} where the operation has been executed. During each state transition, the heterogeneous graph undergoes three transformations. Firstly, the operation node that has been executed is removed, along with all the edges connected to it. Secondly, the edges of the executed job are removed, and new edges are created with the next operation that needs to be performed. Lastly, the features of all nodes and edges are updated.

In Figure 1, an example of an instance and state transition is shown. Blue nodes represent jobs, red nodes represent operations, and green nodes represent machines. The edges are directed, and the values on the edges represent their processing times. In this instance, there are two jobs, j_1 composed of o_1 and o_2 , and j_2 composed of o_3 . o_1 can be processed on machine m_1 in five time units, o_2 on machine m_2 in three time units, and o_3 on m_1 in eight units and on m_2 in five units. The action taken is to select the edge (m_1, j_1) , which corresponds to assigning operation o_1 to machine m_1 . After this action, several steps are performed. First, the node o_1 and all its edges are removed. Then, the edges of node j_1 are updated to correspond to its next operation, o_2 . Finally, the edge of j_2 connected to m_1 is updated because performing an operation on this machine now requires waiting until o_1 is completed.

Reward function. The objective of the agent is to minimize the makespan. As proposed in multiple papers (Zhang et al., 2020a; Lei et al., 2022), one way to minimize the total makespan is by defining the reward function at step t as $r(s_t, a_t, s_{t+1}) = C(s_t) - C(s_{t+1})$, where $C(s_t)$ represents the makespan at step t . If the discount factor, γ is set to 1, the accumulated reward becomes $\sum_{t=0}^{|\mathcal{O}|} r(s_t, a_t, s_{t+1}) = C(s_0) - C(s_{|\mathcal{O}|})$. Assuming that the makespan is zero or a constant in the first step, minimizing the accumulated reward is equivalent to minimizing $C_{s_{|\mathcal{O}|}}$, which is the makespan in the final state.

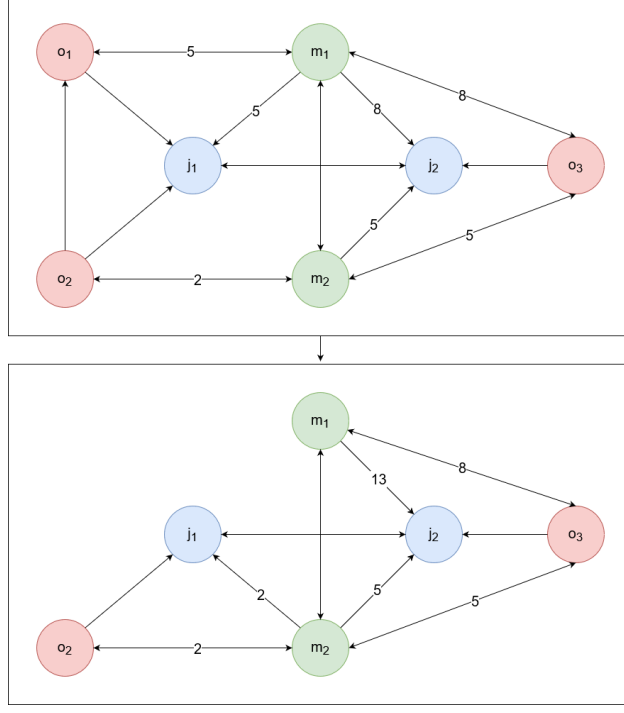


Figure 1: In the top figure, the original FJSSP is represented. In the bottom figure, o_1 has been assigned to m_1 and some edges of the graph have been removed.

4.2 Feature extraction

To extract the state information, which will be used to generate a policy, we employed a GNN that utilizes the attention mechanisms of GATv2 explained in Section 2.3. This approach differs from the one used by Song et al. (2022) and Wang et al. (2023), where they employ a simpler attention mechanism. As demonstrated by Brody et al. (2021), it is possible to obtain GNN architectures with higher and more dynamic attention capacity without significantly increasing the computational cost. This is crucial for a problem such as the FJSSP. For each type of node, the initial representations are denoted as follows: $\mathbf{h}_{j_i} \in \mathbb{R}^{d_{\mathcal{J}}}$ for jobs, $\mathbf{h}_{o_{ij}} \in \mathbb{R}^{d_{\mathcal{O}}}$ for operations, and $\mathbf{h}_{m_i} \in \mathbb{R}^{d_{\mathcal{M}}}$ for machines, where $d_{\mathcal{O}}, d_{\mathcal{J}}, d_{\mathcal{M}}$ are the number of initial features of operations, jobs and machines respectively. The following section describes how the embeddings of the three types of nodes that compose the state are calculated.

Operation embeddings. Each operation receives information from its successor and the machines on which it can be processed. Therefore, it is necessary to calculate two attention weights. For each $o_{ij} \in \mathcal{O}_{j_{i_t}}$ with $j \leq |\mathcal{O}_{j_{i_t}}| - 1$, the weight $e_{o_{ijj+1}}$ between the preceding operations o_{ij} and o_{ij+1} is calculated as:

$$e_{o_{ijj+1}} = \mathbf{a}^{\mathcal{O}\top} \text{LeakyReLU}(\mathbf{W}_1^{\mathcal{O}} \mathbf{h}_{o_{ij}} + \mathbf{W}_2^{\mathcal{O}} \mathbf{h}_{o_{ij+1}}) \quad (7)$$

where $\mathbf{a}^{\mathcal{O}\top} \in \mathbb{R}^{2d'_{\mathcal{O}}}$ and $\mathbf{W}_1^{\mathcal{O}}, \mathbf{W}_2^{\mathcal{O}} \in \mathbb{R}^{d'_{\mathcal{O}} \times d_{\mathcal{O}}}$ are learned linear transformations for all $j \leq |\mathcal{O}_{j_{i_t}}| - 1$ and $d'_{\mathcal{O}}$ is the size of the dimension of the embedding of the operation. We also calculate the attention coefficient between a operation with itself, $e_{o_{ijj}}$. To calculate the attention between the nodes of machines and operations, considering that these edges also have features, we use $e_{om_{ijk}}$ to represent the edge connecting operation o_{ij} and machine m_k , and $\mathbf{h}_{p_{ijk}} \in \mathbb{R}^{d_{\mathcal{O}\mathcal{M}}}$ as the initial representation of the features of that edge. The weight between nodes o_{ij} and m_k is calculated as follows:

$$e_{om_{ijk}} = \mathbf{a}^{\mathcal{O}\mathcal{M}\top} \text{LeakyReLU}(\mathbf{W}_1^{\mathcal{O}\mathcal{M}} \mathbf{h}_{o_{ij}} + \mathbf{W}_2^{\mathcal{O}\mathcal{M}} \mathbf{h}_{m_k} + \mathbf{W}_3^{\mathcal{O}\mathcal{M}} \mathbf{h}_{p_{ijk}}) \quad (8)$$

where $\mathbf{a}^{\mathcal{O}\mathcal{M}\top} \in \mathbb{R}^{3d'_{\mathcal{O}\mathcal{M}}}$ and $\mathbf{W}_1^{\mathcal{O}\mathcal{M}} \in \mathbb{R}^{d'_{\mathcal{O}\mathcal{M}} \times d_{\mathcal{O}}}$, $\mathbf{W}_2^{\mathcal{O}\mathcal{M}} \in \mathbb{R}^{d'_{\mathcal{O}\mathcal{M}} \times d_{\mathcal{M}}}$, $\mathbf{W}_3^{\mathcal{O}\mathcal{M}} \in \mathbb{R}^{d'_{\mathcal{O}\mathcal{M}} \times d_{\mathcal{O}\mathcal{M}}}$. After normalizing the attention weights that the operation has with its successor and itself, and the weight between the operation and the machines where it can be processed using a softmax function, the normalized attention coefficients $\alpha_{o_{ijj}}$, $\alpha_{o_{ijj+1}}$, and $\alpha_{om_{ijk}}$ are obtained, and the new representation of the operation $\mathbf{h}_{o_{ij}}'$ is calculated as follows:

$$\mathbf{h}_{o_{ij}}' = \text{ELU}(\alpha_{o_{ij}} \mathbf{W}_2^{\mathcal{O}} \mathbf{h}_{o_{ij}} + \alpha_{o_{ij+1}} \mathbf{W}_2^{\mathcal{O}} \mathbf{h}_{o_{ij+1}} + \sum_{m_k \in \mathcal{M}_{o_{ij}}} \alpha_{om_{ij}k} (\mathbf{W}_2^{\mathcal{O}\mathcal{M}} \mathbf{h}_{m_k} + \mathbf{W}_3^{\mathcal{O}\mathcal{M}} \mathbf{h}_{p_{ijk}})) \quad (9)$$

Machine embeddings. Machines have two connections from which they will receive information, operations and other machines. The purpose of machines communicating with each other is to be able to understand their state and prioritize their tasks accordingly. The first weight is calculated similarly to $e_{om_{ij}k}$, and it is denoted as e_{m_i, m_j} . To calculate the attention that a machine should assign to other machines, for all $m_i, m_j \in \mathcal{M}$, we compute:

$$e_{m_i, m_j} = \mathbf{a}^{\mathcal{M}\top} \text{LeakyReLU}(\mathbf{W}_1^{\mathcal{M}} \mathbf{h}_{m_i} + \mathbf{W}_2^{\mathcal{M}} \mathbf{h}_{m_j}) \quad (10)$$

where $\mathbf{a}^{\mathcal{M}\top} \in \mathbb{R}^{2d_{\mathcal{M}}}$ and $\mathbf{W}_1^{\mathcal{M}}, \mathbf{W}_2^{\mathcal{M}} \in \mathbb{R}^{d_{\mathcal{M}} \times d_{\mathcal{M}}}$. After normalizing the attention coefficients, \mathbf{h}_{m_i}' is calculated as:

$$\mathbf{h}_{m_i}' = \text{ELU}(\sum_{m_k \in \mathcal{M}} \alpha_{m_i k} \mathbf{W}_2^{\mathcal{M}} \mathbf{h}_{m_k} + \sum_{o_{ij} \in \mathcal{O}_{m_i}} \alpha_{mo_{ij}k} (\mathbf{W}_2^{\mathcal{M}\mathcal{O}} \mathbf{h}_{o_{ij}} + \mathbf{W}_3^{\mathcal{M}\mathcal{O}} \mathbf{h}_{p_{ijk}})) \quad (11)$$

where $\mathbf{W}_2^{\mathcal{M}\mathcal{O}} \in \mathbb{R}^{d_{\mathcal{O}} \times d_{\mathcal{O}}}$, $\mathbf{W}_3^{\mathcal{M}\mathcal{O}} \in \mathbb{R}^{d_{\mathcal{M}\mathcal{O}} \times d_{\mathcal{M}\mathcal{O}}}$.

Job embeddings. The calculation of the embeddings for jobs has three sources of information: the information coming from the operations, the machines, and the other jobs. We define $\mathcal{M}\mathcal{J}_{j_i t}$ as the set of machines that can be assigned the job j_i at a step t and $\mathbf{h}_{pg_{ki}} \in \mathbb{R}^{d_{\mathcal{M}\mathcal{J}}}$ as the initial representation of the features of that edge. In summary, by calculating the attention coefficients in a similar manner to the previously described embeddings, \mathbf{h}_{j_i}' is calculated as

$$\mathbf{h}_{j_i}' = \text{ELU}(\sum_{j_j \in \mathcal{J}} \alpha_{j_i j} \mathbf{W}_2^{\mathcal{J}} \mathbf{h}_{j_j} + \sum_{o_{ij} \in \mathcal{O}_{j_i t}} \alpha_{jo_{ij}} \mathbf{W}_2^{\mathcal{J}\mathcal{O}} \mathbf{h}_{o_{ij}} + \sum_{m_k \in \mathcal{M}\mathcal{J}_{j_i t}} \alpha_{m_j k i} (\mathbf{W}_2^{\mathcal{M}\mathcal{J}} \mathbf{h}_{m_k} + \mathbf{W}_3^{\mathcal{M}\mathcal{J}} \mathbf{h}_{pg_{ki}})) \quad (12)$$

where $\mathbf{W}_2^{\mathcal{J}} \in \mathbb{R}^{d_{\mathcal{J}} \times d_{\mathcal{J}}}$, $\mathbf{W}_2^{\mathcal{J}\mathcal{O}} \in \mathbb{R}^{d_{\mathcal{O}} \times d_{\mathcal{O}}}$, $\mathbf{W}_2^{\mathcal{M}\mathcal{J}} \in \mathbb{R}^{d_{\mathcal{M}} \times d_{\mathcal{M}}}$, $\mathbf{W}_3^{\mathcal{M}\mathcal{J}} \in \mathbb{R}^{d_{\mathcal{M}\mathcal{J}} \times d_{\mathcal{M}\mathcal{J}}}$.

The process just described details how to perform the calculation for the first layer of the GNN. However, this process can be repeated L times, generating the embeddings $\mathbf{h}_{j_i}'^{(L)}$, $\mathbf{h}_{o_{ij}}'^{(L)}$, $\mathbf{h}_{m_k}'^{(L)}$, where each layer uses the embeddings of jobs, operations, and machines from the previous layer, and all layers make use of $\mathbf{h}_{pg_{ki}}$ and $\mathbf{h}_{p_{ijk}}$, i.e., the original edge features.

4.3 Generating a policy

To generate a policy, we employed the well-known PPO algorithm (Schulman et al., 2017). This involves generating a policy (actor) $\pi_{\theta}(a_t | s_t)$ and a value network (critic) $v_{\theta}(s_t)$. Both networks use the embeddings calculated by the GNN, although in different ways. For the policy, we make predictions using the embeddings of the edges $\mathcal{M}\mathcal{J}_t$. For each $(m_k, j_i) \in \mathcal{M}\mathcal{J}_t$, we concatenate the embeddings of the machine $\mathbf{h}_{m_k}'^{(L)}$, the job $\mathbf{h}_{j_i}'^{(L)}$, and the edge feature $\mathbf{h}_{pg_{ki}}$, and then apply $\text{MLP}_{1\theta}$, a mask, that will be presented in the next section, and a softmax function to create a probability distribution over all possible pairs of jobs and machines. For the critic, we apply another $\text{MLP}_{2\theta}$ to all job embeddings, with hyperbolic tangent as the activation function, and perform mean pooling to obtain a single value, as described in the following formula:

$$v_{\theta}(s_t) = \frac{1}{|\mathcal{J}_t|} \sum_{j_i \in \mathcal{J}_t} \text{MLP}_{2\theta}(\mathbf{h}_{j_i}'^{(L)}) \quad (13)$$

To train both networks, we run the policy for n_{eps} episodes, where in each episode, the agent interacts with the environment by sampling from the probability distribution $\pi_{\theta}(a_t | s_t)$, and the experiences are stored in a buffer. A schematic representation of the architecture of our approach is presented in Figure 2. Every n_t episodes, we use these experiences to train the networks for K epochs in batches of size b . Additionally, every n_g episodes, a new set of synthetic instances of dimension n_{ins} is generated for the agent to interact with.

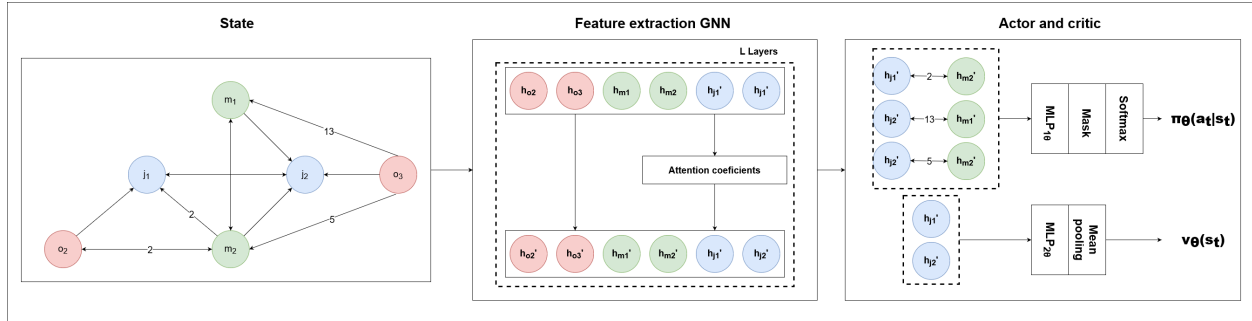


Figure 2: The network architecture of our approach.

4.4 More Robust Inference

In some preliminary experiments, we observed that the results obtained from the generated models were not very robust. Although two models may have similar average results on a benchmark, there can be significant differences between instances within the benchmark. To address this issue, we propose two methods to make our approach more robust.

Dispatching Rules to Limit the Action Space. DRs have been widely used in FJSSP, but their results can be improved, as shown in the next section. However, they serve as a good baseline for the agent’s decision-making by limiting the action space. In this research, we consider two simple heuristics to limit the action space: allowing only the selection of the k operations that can start earlier (if there is a tie, all operations with the same value are allowed) or allowing the k operations that finish earlier. By constraining the action space in this way, we only allow those actions that typically lead to an optimal makespan, as it prevents selecting actions that create large gaps in the scheduling. The value k restricts the degree of freedom the agent has in making decisions. We choose these simple heuristics to avoid excessive computational costs that could increase inference time. Moreover, limiting the action space accelerates the model training by reducing the state space that the agent explores.

Generating a Diverse Set of Scheduling Policies. We propose a method for generating a diverse set of scheduling policies using Bayesian optimization (BO) with the aim of achieving robust results in inference, as a single model may not be robust. First, we define a search space for the BO algorithm, denoted as \mathcal{D} , where we determine which variables to optimize. These variables will be related to the structure of the GNN, the PPO algorithm, the DRs used to limit the action space, or the parameters used to generate the instances. Next, we generate a validation set \mathcal{V} of size $n_{\mathcal{V}}$ and obtain the optimal (or suboptimal) makespan of each instance using exact methods, stored in the set \mathcal{VM} , though the function `get_validation_makespans`(\mathcal{V}). $n_{\mathcal{V}}$ should not be very large to avoid excessive computational cost in the calculation of makespans. For the validation and training of the models, small to medium-sized instances are used, which can be solved without excessive computational cost. We then sample the domain \mathcal{D} using the function `sample`(\mathcal{D}) to obtain hyperparameters d . Using d , we train a policy using the method described in the previous section, implemented in the function `generate_policy`(d). The generated policy is evaluated on \mathcal{V} , and the makespan it produces for each instance is used to calculate the gap compared to the optimal makespan in \mathcal{VM} . For a given instance $v \in \mathcal{V}$, the gap for policy p is computed as $g_{p_v} = \frac{(p_v - \mathcal{VM}_v)}{\mathcal{VM}_v}$, where p_v is the makespan achieved by policy p on instance v and \mathcal{VM}_v is the result obtained using exact methods. These gap calculations are implemented in the function `eval_policy`($\mathcal{V}, \mathcal{VM}, p$). As the first policy is generated, all its results are stored in \mathcal{CG} as the current best gaps achieved. Before starting the BO process, this policy is added to the set of candidate policies to be selected, denoted as \mathcal{C} .

The BO process is executed for n_{BO} iterations. In each iteration $j \in \{1, 2, \dots, n_{BO}\}$, a set of hyperparameters d_j is chosen, and a new policy p_j is generated and evaluated to obtain the gaps \mathcal{G}_{p_j} . The maximum difference between the current gaps and those generated by p_j is calculated. This difference serves as the objective function for the BO algorithm, encouraging the generation of policies that achieve good results on validation instances with more room for improvement. If this difference is positive, it means that the new policy has obtained a better result on at least one instance. Therefore, this new policy is added to the set of candidate policies, and the current gaps are updated.

Once a set of diverse scheduling policies is generated, a subset of these policies is selected to run in parallel during inference. The number of policies to parallelize will be determined based on the available computing capacity. To

accomplish this, the K -Nearest Neighbors algorithm is applied to the validation set results for each policy to group in $n_{\mathcal{P}}$ clusters the policies based on similar outcomes in the validation set. The centroid of each cluster is calculated, and the closest policy, using the euclidian distance, within each cluster is selected as a final candidate, using the function `cluster_center`(\mathcal{K}, \mathcal{C}), and generating the set of policies \mathcal{P} that will be parallelized during inference. This approach ensures that similar policies are not executed in inference. The algorithm for creating a diverse set of scheduling policies (DSP) is shown in Algorithm 1.

Algorithm 1 Algorithm to generate a set of diverse scheduling policies.

Input: BO domain \mathcal{D} , BO iterations n_{BO} , number of policies $n_{\mathcal{P}}$, validation set size $n_{\mathcal{V}}$
Output: Policies \mathcal{P}

- 1: **function** DSP($\mathcal{D}, n_{\mathcal{P}}, n_B, n_{\mathcal{V}}$)
- 2: Generate a validation set \mathcal{V}
- 3: $\mathcal{VM} \leftarrow \text{get_validation_makespans}(\mathcal{V})$
- 4: $d \leftarrow \text{sample}(\mathcal{D})$
- 5: $p \leftarrow \text{generate_policy}(d)$
- 6: $\mathcal{CG} \leftarrow \text{eval_policy}(\mathcal{V}, \mathcal{VM}, p)$
- 7: $\mathcal{C} \leftarrow \{p\}$
- 8: **for** $j = 1$ to n_{BO} **do**
- 9: $d_j \leftarrow \text{sample}(\mathcal{D})$
- 10: $p_j \leftarrow \text{generate_policy}(d_j)$
- 11: $\mathcal{G}_{p_j} \leftarrow \text{eval_policy}(\mathcal{V}, \mathcal{VM}, p_j)$
- 12: $g_j \leftarrow \max(\mathcal{CG} - \mathcal{G}_{p_j})$
- 13: **if** $g_j > 0$ **then**
- 14: $\mathcal{C} \leftarrow \mathcal{C} \cup \{p_j\}$
- 15: $\mathcal{CG}_v \leftarrow \min_{v \in \mathcal{V}}(\mathcal{CG}_v, \mathcal{G}_{p_{jv}})$
- Update surrogate model with (d_j, g_j)
- 16: $\mathcal{K} \leftarrow \text{KNN}(\mathcal{C}, n_{\mathcal{P}})$
- 17: $\mathcal{P} \leftarrow \text{cluster_center}(\mathcal{K}, \mathcal{C})$
- return** \mathcal{P}

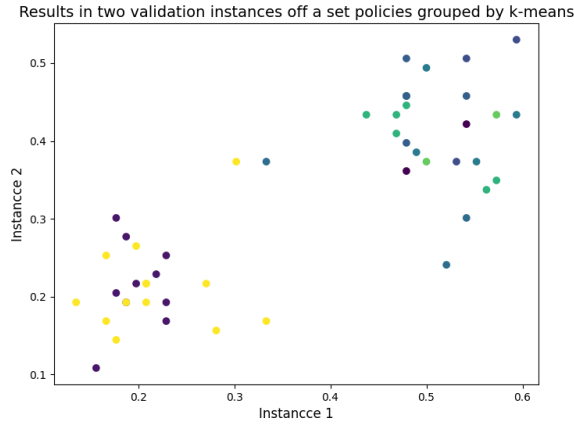


Figure 3: The gap of two instances of the validation set of all the generated candidate policies is shown, colored by the cluster they belong to. All the policies have been divided into 9 clusters. It can be observed that the yellow and purple clusters achieve the best results for these two instances.

5 Experimental results

In this section, we present the experiments conducted to evaluate the validity of the proposed methodology, which we refer to as Diverse Scheduling Policies (DSP), we study its capability to outperform DRs and its competitiveness with other state-of-the-art approaches. For this purpose, comparisons have been made with synthetically generated instances

and publicly available FJSSP benchmarks ², measuring both the quality of the solutions and the time required. The method was implemented using Python 3.10, PyTorch Geometric (Fey and Lenssen, 2019) was utilized for GNNs, Optuna (Akiba et al., 2019) was used for hyperparameter optimization and OR-Tools for the exact method ³. The hardware is a machine with AMD Ryzen 5 5600X processor and an NVIDIA GeForce RTX 3070 Ti. The code and the synthetically generated test instances will be made publicly available upon acceptance of the paper.

5.1 Generation of Synthetic Instances

To train the models, synthetic instances must be generated, and for this purpose, the instance generation method proposed in Brandimarte (1993) and Song et al. (2022) has been adapted. The generation of synthetic instances is governed by various parameters that determine their size and structure. These parameters include the minimum and maximum number of jobs (j_{\min} and j_{\max}), the minimum and maximum number of machines (m_{\min} and m_{\max}), the minimum and maximum number of operations per job (o_{\min} and o_{\max}), the maximum number of options each operation can have (op_{\max} , with a minimum fixed at four), the maximum processing time for an operation \bar{p} (with a minimum defined as one), and the deviation from the mean d . To generate an instance, the uniform distribution within the defined ranges is sampled. The processing time on machine m_k is calculated by sampling from the uniform distribution $\mathcal{U}(\bar{p}_{i\bar{j}}(1-d), \bar{p}_{i\bar{j}}(1+d))$. Training on large instances can be time-consuming, so smaller instances are used for that purpose, while larger instances are used for testing.

5.2 Configuration

For the experiments, the validation set size, $n_{\mathcal{V}}$, has been set to 100, the number of BO iterations n_{BO} has been set to 200 and the synthetic instances have been generated by randomly selecting from the number of jobs, machines and operation ranges defined below. Tree-structured Parzen Estimator has been used as the sampler. The size of the policy set $n_{\mathcal{P}}$ has been set to 6, to enable efficient parallelization of the models. Regarding the domain of BO, the hyperparameters can be divided into categories related to: the structure of the GNN, the training mode of the PPO algorithm, the size of the generated instances, and the heuristic and degrees of freedom for decision-making. The following ranges have been considered:

- Related to the GNN: the number of layers $L \in [1, 3]$ and the number of hidden channels $d' \in \{32, 64, 128\}$. For simplicity, the dimension of the node embeddings has been considered the same for all nodes. $MLP_{1\theta}$ and $MLP_{2\theta}$ of the actor and the critic have a single layer of the same dimension.
- The defined ranges for generating instance sets in each iteration of BO were: $j_{\min} \in [5, 9]$, $j_{\max} \in [10, 15]$, $m_{\min} \in [4, 7]$, $m_{\max} \in [9, 13]$, $op_{\max} \in [5, 9]$, $p \in [8, 25]$. d has been set to 0.2.
- Related to network training: the maximum number of episodes during training $n_{\text{eps}} \in [10000, 20000]$, learning rate $lr \in [0.00001, 0.001]$, batch size $b \in \{64, 128, 256\}$, model training frequency $n_t \in [10, 100]$, and frequency of creating new instances $n_{\text{ins}} \in [1, 10]$.
- The heuristic used by the environment, as well as the possible options $k \in [1, 3]$.

Allowing the BO algorithm to have many hyperparameter options aims to obtain diverse models that can be effective on different subsets of instances. For the PPO algorithm, the discount factor γ was fixed to 1, the clipping parameter ϵ to 0.2, and the coefficients for policy, value, and entropy in the loss function were set to 1, 0.5, and 0.01, respectively. The number of epochs per episode was set to 3, and Adam optimizer (Kingma and Ba, 2014) was used.

5.3 Results in synthetically generated instances

First, we have validated our approach by comparing it with various well-known DRs. Additionally, optimal or near-optimal solutions have been generated using OR-Tools, running it for 1800 seconds, using the CP-SAT solver. OR-Tools has been used in multiple papers for this purpose (Song et al., 2022; Wang et al., 2023; Tassel et al., 2021), because it is one of the best open-source tools for solving scheduling problems (Da Col and Teppan, 2019). The objective is to study if our approach outperforms the DRs, as their execution times are similar to our method, and to measure the gap between the solution obtained by our approach and the optimal solution. For this purpose, four sets of instances larger than the instances used during the training phase have been generated. The metrics used to measure the results have been the gap between the method and the solution proposed by OR-Tools (the lower the value, the better,

²We obtained the benchmarks from <https://openhsu.ub.hsu-hh.de/handle/10.24405/436>.

³We obtained the implementation from https://github.com/google/or-tools/blob/stable/examples/python/flexible_job_shop_sat.py.

and a negative value indicates that it is better than OR-Tools), and the execution time.

Regarding the heuristic rules that have been used, they have been shown to be effective in the literature (Jun et al., 2019) and have recently been used to compare them with other deep learning-based methods (Lei et al., 2022; Chen and Matis, 2013). To define a heuristic for solving the FJSSP, two rules need to be defined: one for job selection and sequencing, and another for operation assignment to machines. Regarding the former, the following rules have been considered:

- First In First Out (FIFO), which processes the first operation to arrive in the queue of a machine.
- Most Work Remaining (MWKR), which processes a job with the highest remaining workload.
- Least Work Remaining (LWKR), which processes a job with the lowest remaining workload.
- Most Operation Number Remaining (MOPNR), which processes a job with the highest number of remaining operations.

For the machine selection criteria, the following rules have been considered:

- Shortest Processing Time (SPT), which assigns a machine with the shortest processing time for an operation.
- Earliest Ending Time (EET), which selects the machine where an operation can start earliest.

To compare our method, we generated four sets of instances, each consisting of 50 instances, which are larger than the ones used to train our model. The creation of these sets followed an incremental approach, where they became progressively more complex. The parameters used for each set are detailed in Table 1. For the first test set, \mathcal{S}_1 , we doubled the number of jobs and operations compared to the ones used in the training set. In \mathcal{S}_2 , we increased the number of jobs and the processing times, allowing for more extensive and unseen ranges during the training phase. In \mathcal{S}_3 , we further increased the number of jobs and, finally, in \mathcal{S}_4 , we increased the number of possible machines.

Table 1: Summary of the size of the test instances

Name	Range jobs	Range machines	Ops per job	Processing time
\mathcal{S}_1	$\mathcal{U}(20, 30)$	$\mathcal{U}(8, 16)$	$\mathcal{U}(4, 8)$	$\mathcal{U}(1, 7)$
\mathcal{S}_2	$\mathcal{U}(40, 50)$	$\mathcal{U}(8, 16)$	$\mathcal{U}(4, 8)$	$\mathcal{U}(5, 20)$
\mathcal{S}_3	$\mathcal{U}(50, 60)$	$\mathcal{U}(8, 16)$	$\mathcal{U}(4, 8)$	$\mathcal{U}(5, 20)$
\mathcal{S}_4	$\mathcal{U}(50, 60)$	$\mathcal{U}(16, 32)$	$\mathcal{U}(8, 16)$	$\mathcal{U}(5, 20)$

In Table 2, the average gaps and execution times obtained by the eight DRs and our approach are shown for the synthetically generated test sets. As can be observed, although our approach takes slightly more time, it consistently outperforms the eight DRs. Furthermore, the performance of our proposed method is more robust than that of the DRs as the problem scales increases. More interestingly, the results obtained for large instances are better than those obtained by OR-Tools (as the gap achieved is negative), although the execution time of our methods is much less. This demonstrates that our approach has been able to generalize the knowledge learned from small instances to larger instances with more machines, jobs, operations, and average processing times.

Table 2: Summary of the result in test instances of all DRs and our approach (DSP) with respect to OR-Tools.

Name	Obj.	FIFO		LWKR		MWKR		MOPNR		DSP	OR-Tools
		EET	SPT	EET	SPT	EET	SPT	EET	SPT		
\mathcal{S}_1	Gap(%)	27.28	61.30	92.56	86.03	26.05	52.80	28.08	53.36	10.84	-
	Time(s)	0.11	0.13	0.13	0.13	0.13	0.14	0.14	0.13	8.54	1591.63
\mathcal{S}_2	Gap(%)	13.40	33.25	58.24	48.07	12.07	30.62	13.25	32.29	6.96	-
	Time(s)	0.26	0.30	0.29	0.28	0.27	0.29	0.29	0.34	32.90	1800.38
\mathcal{S}_3	Gap(%)	10.36	27.56	50.31	36.93	9.95	26.35	10.77	26.41	6.05	-
	Time(s)	0.36	0.40	0.36	0.37	0.37	0.39	0.39	0.43	57.61	1800.45
\mathcal{S}_4	Gap(%)	7.43	29.99	95.92	69.29	4.43	26.82	7.85	26.11	-3.06	-
	Time(s)	0.94	1.08	0.93	0.98	0.97	0.95	1.04	1.08	166.56	1801.52

5.4 Results in publicly available FJSSP benchmarks

To study the generalization capability of the proposed method on real-world instances, 45 large instances from the Behnke benchmark (Behnke and Geiger, 2012) have been used and, although our main focus is large instances, we have also used the instances proposed by Hurink et al. (1994) (40 small and medium-sized instances from the vdata set) to assess that there still is a competitive alternative for small ones. We have chosen these subsets from these benchmarks in order to compare our results with the approach presented by Lei et al. (2022). In addition to comparing it with this approach, we compare our method with the methods proposed by Wang et al. (2023) and Song et al. (2022), both also recent DRL methods, using their publicly available open-source code and using their default settings to train and test the models. To perform the inference, the sampling strategy has been used, as described in Song et al. (2022). This strategy involves running the instance 100 times by sampling from the distribution π_θ instead of selecting the maximum probability, and choosing the smallest makespan value among all runs. This strategy has been chosen because it yields better results than selecting the maximum probability from π_θ , which is called the greedy approach. In each benchmark, we have also compared the DRL methods with the best DR among the proposed ones.

Results in vdata benchmark. Table 3 shows the results obtained by the four methods grouped according to the size of the instances. Since the optimal or sub-optimal solutions for these instances are available, as published by Behnke and Geiger (2012), we will use them instead of OR-Tools in this case, and also because the other approaches also use them. Nevertheless, the results obtained with OR-Tools are very similar to those obtained from Behnke and Geiger (2012).

Table 3: Comparison of the mean gap grouped by size obtained by DRs, the methods proposed by Song et al., Wang et al. and Lei et al. and our approach (DSP) in vdata instances.

Size	Obj.	DR	Song	Wang	Lei	DSP
10x5	Gap(%)	41.40	6.89	3.09	8.00	4.14
	Time (s.)	0.03	4.79	0.72	-	2.67
10x10	Gap(%)	49.38	0.28	0.27	0.32	1.24
	Time (s.)	0.06	9.10	1.75	-	2.77
15x5	Gap(%)	30.34	2.99	1.13	3.24	2.10
	Time (s.)	0.04	6.38	1.05	-	2.38
15x10	Gap(%)	63.06	7.35	5.13	11.44	4.07
	Time (s.)	0.10	13.19	3.47	-	4.17
15x15	Gap(%)	57.26	0.88	0.88	3.25	0.91
	Time (s.)	0.16	24.11	7.85	-	7.52
20x5	Gap(%)	24.32	2.97	0.94	1.85	0.88
	Time (s.)	0.07	7.90	1.58	-	2.92
20x10	Gap(%)	50.01	5.02	1.79	4.08	1.50
	Time (s.)	0.14	18.14	5.29	-	6.11
30x10	Gap(%)	33.08	3.25	1.16	1.91	0.57
	Time (s.)	0.27	30.36	11.48	-	12.10

As expected, the results of the best DR, which is FIFO for job selection and EET for machine selection, yield the worst results. Regarding the DRL-based methods, all three of them achieve a similar average gap, with the best mean gap achieved by Wang et al. (2023), 1.81%. Our DSP method follows closely with the second-best results, featuring an average gap of 1.94% nearly identical to the previous. This is followed by the method of Song et al. (2022) at 3.72% and Lei et al. (2022) at 4.27%. We emphasize that, as seen in Table 3, the average results for larger instances are better with our method, suggesting that our approach is more robust with this kind of instances. We speculate that the better outcomes in smaller instances by Wang et al. (2023) may be attributed to their state representation featuring more features and their GNN utilizing a dual attention heads architecture. As for the average execution times, which are shown in Table 3, we compared the proposed methods except for the one by Lei et al. (2022) as they did not provide their exact times. As can be seen in Table 3, the DRL-based methods achieve similar execution times.

Results in Behnke benchmark. Table 4 shows the results grouped according to the size of the instances from the benchmark obtained by the best DR, the four DRL methods, and OR-Tools, which was used to obtain pseudo-optimal results by running it for 1800 seconds. In A, the results for each of the instances are displayed. It is important to show the results obtained by the solver on each instance because, for example, in comparison, Lei et al. (2022) achieve their results by running the Gurobi solver for 3600 seconds and obtain considerably worse results.

In this case, our approach outperforms Wang et al. (2023) in 40 out of 45 instances, Lei et al. (2022) in 34 and Song et al. (2022) and the DRs in all instances. Furthermore, our approach performs better on more challenging instances. In terms of the average gap, notable differences exist among the DRL methods in this benchmark. The method proposed by Song et al. (2022) achieves the worst results among the DRL methods, 38.48%, close to the DRs, 55.65%, indicating instability issues for large instances. The other two DRL approaches are more robust, although our method, 2.91%, is clearly superior to those proposed by Lee et al. (2021), 7.27%, and Wang et al. (2023), 6.42%. Regarding execution time, as shown in Table 4, it can be observed that as the instance dimension increases, the processing time significantly especially increases for especially Wang et al. (2023), which is slower than our approach. This could be because they calculate more features, particularly within the operation-type nodes, which are more numerous.

Table 4: Comparison of the mean gap grouped by size obtained by DRs, the methods proposed by Song et al., Wang et al. and Lei et al. and our approach (DSP) in Behnke instances.

Size	Obj.	DR	Song	Wang	Lei	DSP	OR-Tools
20x20	Gap(%)	74.07	42.65	17.55	11.93	10.53	-
	Time (s.)	0.08	10.29	2.78	-	3.60	1481.77
20x40	Gap(%)	69.09	50.57	13.86	16.19	12.53	-
	Time (s.)	0.09	11.39	6.43	-	6.67	607.57
20x60	Gap(%)	67.38	50.22	14.36	20.23	12.64	-
	Time (s.)	0.10	14.38	12.35	-	12.06	539.37
50x20	Gap(%)	62.98	34.44	8.11	0.01	1.94	-
	Time (s.)	0.33	29.16	14.63	-	15.26	1800.30
50x40	Gap(%)	54.14	40.59	7.15	11.88	3.27	-
	Time (s.)	0.36	30.67	37.505	-	26.07	1800.57
50x60	Gap(%)	53.19	44.09	6.13	12.27	3.78	-
	Time (s.)	0.39	37.82	65.824	-	41.53	1800.83
100x20	Gap(%)	44.03	23.70	-4.73	-11.02	-9.36	-
	Time (s.)	1.12	68.88	54.794	-	61.05	1800.62
100x40	Gap(%)	38.63	28.21	-2.69	2.03	-4.95	-
	Time (s.)	1.27	82.27	134.12	-	93.44	1801.15
100x60	Gap(%)	37.37	31.85	-1.92	1.92	-4.21	-
	Time (s.)	1.28	102.07	235.10	-	130.15	1801.69

6 Conclusions and future work

This paper has introduced a novel method based on DRL and GNNs to dynamically and robustly solve the FJSSP. To achieve this, we first proposed a new representation of states, action space, and transition function, where nodes and edges are progressively removed to make our method more efficient. Secondly, we designed a message passing scheme between nodes and a more expressive attention mechanism, not employed by other methods in the literature. Moreover, we presented two new approaches to enhance inference, making it more robust. This was achieved by creating a set of diverse policies that can be executed in parallel and by constraining the action space using DRs, resulting in faster model training and more robust inference.

To validate our approach, we generated new instances larger than those used in the training phase, demonstrating the generalization capability of our architecture. The results revealed that our method outperforms eight DRs on large instances. Furthermore, we compared our method with public benchmarks and recent DRL-based approaches. In small to medium-sized instances, our method outperformed two of the three methods and was slightly worse than the third. In large instances, it significantly outperformed all three methods. Notably, our method even outperformed OR-Tools on instances with a higher number of jobs and machines, all while maintaining significantly lower execution times.

For future work, we plan to extend this method to handle additional complexities in the FJSSP, such as new job insertions or setup times. Moreover, we aim to apply our approach to the low-carbon FJSSP, which considers both the makespan and energy consumption of machines. Additionally, it will be interesting to study the possibility to extend this approach to other combinatorial optimization and operations research problems, such as hub location problems or knapsack problems.

Acknowledgements

This work was partially financed by the Basque Government through their Elkartek program (SONETO project, ref. KK-2023/00038). R. Santana thanks the Misiones Euskampus 2.0 programme for the financial help received through Euskampus Fundazioa. Partial support by the Research Groups 2022-2024 (IT1504-22) and the Elkartek Program (KK-2020/00049, KK-2022/00106, SIGZE, K-2021/00065) from the Basque Government, and the PID2019-104966GB-I00 and PID2022-137442NB-I00 research projects from the Spanish Ministry of Science is acknowledged.

References

- Akiba, T., Sano, S., Yanase, T., Ohta, T., Koyama, M., 2019. Optuna: A next-generation hyperparameter optimization framework, in: *Proceedings of the 25th ACM SIGKDD International Conference on Knowledge Discovery & Data Mining*, pp. 2623–2631.
- Balas, E., 1969. Machine sequencing via disjunctive graphs: an implicit enumeration algorithm. *Operations Research* 17, 941–957.
- Behnke, D., Geiger, M.J., 2012. Test instances for the flexible job shop scheduling problem with work centers. *Arbeitspapier/Research Paper/Helmut-Schmidt-Universität, Lehrstuhl für Betriebswirtschaftslehre, insbes. Logistik-Management*.
- Brandimarte, P., 1993. Routing and scheduling in a flexible job shop by tabu search. *Annals of Operations Research* 41, 157–183.
- Brody, S., Alon, U., Yahav, E., 2021. How attentive are graph attention networks? *arXiv preprint arXiv:2105.14491*.
- Çalış, B., Bulkan, S., 2015. A research survey: review of AI solution strategies of job shop scheduling problem. *Journal of Intelligent Manufacturing* 26, 961–973.
- Calleja, G., Pastor, R., 2014. A dispatching algorithm for flexible job-shop scheduling with transfer batches: an industrial application. *Production Planning & Control* 25, 93–109.
- Cappart, Q., Moisan, T., Rousseau, L.M., Prémont-Schwarz, I., Cire, A.A., 2021. Combining reinforcement learning and constraint programming for combinatorial optimization, in: *Proceedings of the AAAI Conference on Artificial Intelligence*, pp. 3677–3687.
- Chen, B., Matis, T.I., 2013. A flexible dispatching rule for minimizing tardiness in job shop scheduling. *International Journal of Production Economics* 141, 360–365.
- Chen, R., Yang, B., Li, S., Wang, S., 2020. A self-learning genetic algorithm based on reinforcement learning for flexible job-shop scheduling problem. *Computers & Industrial Engineering* 149, 106778.
- Da Col, G., Teppan, E.C., 2019. Industrial size job shop scheduling tackled by present day cp solvers, in: *Principles and Practice of Constraint Programming: 25th International Conference, CP 2019, Stamford, CT, USA, September 30–October 4, 2019, Proceedings* 25, Springer. pp. 144–160.
- Defersha, F.M., Obimuyiwa, D., Yimer, A.D., 2022. Mathematical model and simulated annealing algorithm for setup operator constrained flexible job shop scheduling problem. *Computers & Industrial Engineering* 171, 108487.
- Du, Y., Li, J., Li, C., Duan, P., 2022. A reinforcement learning approach for flexible job shop scheduling problem with crane transportation and setup times. *IEEE Transactions on Neural Networks and Learning Systems*.
- Fey, M., Lenssen, J.E., 2019. Fast graph representation learning with PyTorch Geometric, in: *ICLR Workshop on Representation Learning on Graphs and Manifolds*.
- Garey, M.R., Johnson, D.S., Sethi, R., 1976. The complexity of flowshop and jobshop scheduling. *Mathematics of Operations Research* 1, 117–129.
- Gupta, A.K., Sivakumar, A.I., 2006. Job shop scheduling techniques in semiconductor manufacturing. *The International Journal of Advanced Manufacturing Technology* 27, 1163–1169.
- Hajibabaei, M., Behnamian, J., 2021. Flexible job-shop scheduling problem with unrelated parallel machines and resources-dependent processing times: A tabu search algorithm. *International Journal of Management Science and Engineering Management* 16, 242–253.
- Hurink, J., Jurisch, B., Thole, M., 1994. Tabu search for the job-shop scheduling problem with multi-purpose machines. *Operations-Research-Spektrum* 15, 205–215.
- Joe, W., Lau, H.C., 2020. Deep reinforcement learning approach to solve dynamic vehicle routing problem with stochastic customers, in: *Proceedings of the International Conference on Automated Planning and Scheduling*, pp. 394–402.

-
- Jun, S., Lee, S., Chun, H., 2019. Learning dispatching rules using random forest in flexible job shop scheduling problems. *International Journal of Production Research* 57, 3290–3310.
- Kim, M.S., Oh, S.C., Chang, E.H., Lee, S., Wells, J.W., Arinez, J., Jang, Y.J., 2022. A dynamic programming-based heuristic algorithm for a flexible job shop scheduling problem of a matrix system in automotive industry, in: 2022 IEEE 18th International Conference on Automation Science and Engineering (CASE), IEEE. pp. 777–782.
- Kingma, D.P., Ba, J., 2014. Adam: A method for stochastic optimization. arXiv preprint arXiv:1412.6980 .
- Lee, K., Laskin, M., Srinivas, A., Abbeel, P., 2021. Sunrise: A simple unified framework for ensemble learning in deep reinforcement learning, in: International Conference on Machine Learning, PMLR. pp. 6131–6141.
- Lei, K., Guo, P., Zhao, W., Wang, Y., Qian, L., Meng, X., Tang, L., 2022. A multi-action deep reinforcement learning framework for flexible job-shop scheduling problem. *Expert Systems with Applications* 205, 117796.
- Lin, C.C., Deng, D.J., Chih, Y.L., Chiu, H.T., 2019. Smart manufacturing scheduling with edge computing using multiclass deep q network. *IEEE Transactions on Industrial Informatics* 15, 4276–4284.
- Liu, C.L., Chang, C.C., Tseng, C.J., 2020. Actor-critic deep reinforcement learning for solving job shop scheduling problems. *IEEE Access* 8, 71752–71762.
- Luo, S., 2020. Dynamic scheduling for flexible job shop with new job insertions by deep reinforcement learning. *Applied Soft Computing* 91, 106208.
- Luo, S., Zhang, L., Fan, Y., 2021. Dynamic multi-objective scheduling for flexible job shop by deep reinforcement learning. *Computers & Industrial Engineering* 159, 107489.
- Manne, A.S., 1960. On the job-shop scheduling problem. *Operations Research* 8, 219–223.
- Mazyavkina, N., Sviridov, S., Ivanov, S., Burnaev, E., 2021. Reinforcement learning for combinatorial optimization: A survey. *Computers & Operations Research* 134, 105400.
- Meng, L., Zhang, C., Ren, Y., Zhang, B., Lv, C., 2020. Mixed-integer linear programming and constraint programming formulations for solving distributed flexible job shop scheduling problem. *Computers & Industrial Engineering* 142, 106347.
- Scarselli, F., Gori, M., Tsoi, A.C., Hagenbuchner, M., Monfardini, G., 2008. The graph neural network model. *IEEE Transactions on Neural Networks* 20, 61–80.
- Schulman, J., Wolski, F., Dhariwal, P., Radford, A., Klimov, O., 2017. Proximal policy optimization algorithms. arXiv preprint arXiv:1707.06347 .
- Song, W., Chen, X., Li, Q., Cao, Z., 2022. Flexible job-shop scheduling via graph neural network and deep reinforcement learning. *IEEE Transactions on Industrial Informatics* 19, 1600–1610.
- Sutton, R.S., Barto, A.G., 2018. Reinforcement Learning: An introduction. MIT press.
- Tassel, P., Gebser, M., Schekotihin, K., 2021. A reinforcement learning environment for job-shop scheduling. arXiv preprint arXiv:2104.03760 .
- Tolstaya, E., Paulos, J., Kumar, V., Ribeiro, A., 2021. Multi-robot coverage and exploration using spatial graph neural networks, in: 2021 IEEE/RSJ International Conference on Intelligent Robots and Systems (IROS), IEEE. pp. 8944–8950.
- Tutumlu, B., Saraç, T., 2023. A mip model and a hybrid genetic algorithm for flexible job-shop scheduling problem with job-splitting. *Computers & Operations Research* 155, 106222.
- Vaswani, A., Shazeer, N., Parmar, N., Uszkoreit, J., Jones, L., Gomez, A.N., Kaiser, Ł., Polosukhin, I., 2017. Attention is all you need. *Advances in Neural Information Processing Systems* 30.
- Veličković, P., Cucurull, G., Casanova, A., Romero, A., Lio, P., Bengio, Y., 2017. Graph attention networks. arXiv preprint arXiv:1710.10903 .
- Wang, R., Wang, G., Sun, J., Deng, F., Chen, J., 2023. Flexible job shop scheduling via dual attention network based reinforcement learning. arXiv preprint arXiv:2305.05119 .
- Wu, Z., Pan, S., Chen, F., Long, G., Zhang, C., Philip, S.Y., 2020. A comprehensive survey on graph neural networks. *IEEE Transactions on Neural Networks and Learning Systems* 32, 4–24.
- Xiong, H., Shi, S., Ren, D., Hu, J., 2022. A survey of job shop scheduling problem: The types and models. *Computers & Operations Research* 142, 105731.
- Zhang, C., Song, W., Cao, Z., Zhang, J., Tan, P.S., Chi, X., 2020a. Learning to dispatch for job shop scheduling via deep reinforcement learning. *Advances in Neural Information Processing Systems* 33, 1621–1632.

-
- Zhang, G., Hu, Y., Sun, J., Zhang, W., 2020b. An improved genetic algorithm for the flexible job shop scheduling problem with multiple time constraints. *Swarm and Evolutionary Computation* 54, 100664.
- Zhang, X.M., Liang, L., Liu, L., Tang, M.J., 2021. Graph neural networks and their current applications in bioinformatics. *Frontiers in Genetics* 12, 690049.
- Zhou, J., Cui, G., Hu, S., Zhang, Z., Yang, C., Liu, Z., Wang, L., Li, C., Sun, M., 2020. Graph neural networks: A review of methods and applications. *AI Open* 1, 57–81.

A Behnke results

In the following table, the results obtained by the different methods and OR-Tools are shown. The gap relative to OR-Tools is presented in parentheses as a percentage.

Table 5: Comparison of the best makespan obtained by DRs, the methods proposed by Song et al., Wang et al. and Lei et al., our approach (DSP) and OR-Tools in instances.

Index	Size	DR	Song	Wang	Lei	DSP	OR
06	20x20	176 (64.84)	179 (39.84)	148 (15.62)	143 (11.72)	141 (10.16)	128
07	20x20	174 (65.89)	176 (36.43)	152 (17.83)	142 (10.08)	138 (6.98)	129
08	20x20	200 (83.33)	185 (46.83)	148 (17.46)	139 (10.32)	142 (12.7)	126
09	20x20	169 (83.2)	180 (44.0)	147 (17.6)	144 (15.2)	142 (13.6)	125
10	20x20	181 (73.08)	190 (46.15)	155 (19.23)	146 (12.31)	142 (9.23)	130
11	50x20	321 (59.53)	337 (31.13)	276 (7.39)	250 (-2.72)	251 (-2.33)	257
12	50x20	282 (57.37)	336 (33.86)	267 (6.37)	247 (-1.59)	250 (-0.4)	251
13	50x20	315 (67.34)	343 (38.31)	271 (9.27)	249 (0.4)	265 (6.85)	248
14	50x20	352 (66.14)	342 (36.25)	275 (9.56)	257 (2.39)	258 (2.79)	251
15	50x20	324 (64.54)	333 (32.67)	271 (7.97)	255 (1.59)	258 (2.79)	251
16	100x20	547 (45.06)	598 (23.05)	460 (-5.35)	437 (-10.08)	444 (-8.64)	486
17	100x20	562 (50.32)	597 (25.68)	449 (-5.47)	430 (-9.47)	439 (-7.58)	475
18	100x20	524 (42.68)	600 (25.52)	466 (-2.51)	428 (-10.46)	440 (-7.95)	478
19	100x20	539 (41.19)	594 (21.72)	468 (-4.1)	423 (-13.32)	436 (-10.66)	488
20	100x20	524 (40.91)	593 (22.52)	454 (-6.2)	427 (-11.78)	426 (-11.98)	484
26	20x40	167 (74.34)	173 (53.1)	132 (16.81)	129 (14.16)	126 (11.5)	113
27	20x40	176 (64.23)	180 (46.34)	137 (11.38)	140 (13.82)	140 (13.82)	123
28	20x40	152 (71.93)	182 (59.65)	132 (15.79)	133 (16.67)	121 (6.14)	114
29	20x40	145 (64.96)	177 (51.28)	131 (11.97)	138 (17.95)	134 (14.53)	117
30	20x40	185 (70.0)	171 (42.5)	136 (13.33)	142 (18.33)	140 (16.67)	120
31	50x40	306 (55.08)	326 (38.14)	253 (7.2)	271 (14.83)	242 (2.54)	236
32	50x40	287 (56.17)	326 (38.72)	254 (8.09)	267 (13.62)	241 (2.55)	235
33	50x40	274 (51.28)	314 (34.19)	248 (5.98)	261 (11.54)	247 (5.56)	234
34	50x40	280 (53.02)	338 (45.69)	250 (7.76)	250 (7.76)	239 (3.02)	232
35	50x40	290 (55.16)	326 (46.19)	238 (6.73)	249 (11.66)	229 (2.69)	223
36	100x40	500 (44.21)	575 (33.1)	429 (-0.69)	442 (2.31)	414 (-4.17)	432
37	100x40	504 (37.19)	567 (26.28)	428 (-4.68)	444 (-1.11)	423 (-5.79)	449
38	100x40	490 (35.51)	570 (28.09)	427 (-4.04)	454 (2.02)	422 (-5.17)	445
39	100x40	498 (39.6)	574 (28.41)	432 (-3.36)	471 (5.37)	412 (-7.83)	447
40	100x40	518 (36.64)	567 (25.17)	450 (-0.66)	460 (1.55)	445 (-1.77)	453
46	20x60	176 (74.56)	172 (50.88)	130 (14.04)	145 (27.19)	131 (14.91)	114
47	20x60	152 (61.54)	177 (51.28)	131 (11.97)	144 (23.08)	127 (8.55)	117
48	20x60	165 (64.0)	182 (45.6)	143 (14.4)	141 (12.8)	142 (13.6)	125
49	20x60	157 (72.57)	171 (51.33)	131 (15.93)	134 (18.58)	126 (11.5)	113
50	20x60	170 (64.23)	187 (52.03)	142 (15.45)	147 (19.51)	141 (14.63)	123
51	50x60	280 (50.44)	328 (45.13)	238 (5.31)	253 (11.95)	240 (6.19)	226
52	50x60	287 (52.65)	323 (42.92)	236 (4.42)	242 (7.08)	233 (3.1)	226
53	50x60	280 (55.41)	323 (45.5)	236 (6.31)	256 (15.32)	231 (4.05)	222
54	50x60	302 (55.7)	343 (44.73)	251 (5.91)	268 (13.08)	243 (2.53)	237
55	50x60	297 (51.74)	327 (42.17)	250 (8.7)	262 (13.91)	237 (3.04)	230
56	100x60	499 (36.64)	569 (31.11)	425 (-2.07)	439 (1.15)	411 (-5.3)	434
57	100x60	526 (43.29)	565 (30.79)	427 (-1.16)	442 (2.31)	412 (-4.63)	432
58	100x60	475 (34.09)	592 (34.55)	428 (-2.73)	442 (0.45)	424 (-3.64)	440
59	100x60	458 (36.26)	567 (30.95)	426 (-1.62)	443 (2.31)	424 (-2.08)	433
60	100x60	493 (36.57)	584 (31.83)	434 (-2.03)	458 (3.39)	419 (-5.42)	443
Mean Gap (%)		55.65	38.48	6.42	7.27	2.91	